Functional Loss in the Magnocellular and Parvocellular Pathways in Patients with

Optic Neuritis

Dingcai Cao[1], Andrew J. Zele[2], Joel Pokorny[3], David Y. Lee[4], Leonard V. Messner[4], Christopher Diehl[4], Susan Ksiazek[1]

[1] Department of Ophthalmology & Visual Sciences, University of Illinois at Chicago,

Chicago, IL, USA

[2] Institute of Health and Biomedical Innovation & School of Optometry, Queensland

University of Technology, Brisbane, Australia

[3] Visual Science Laboratories, University of Chicago, Chicago, IL, USA

[4] Illinois College of Optometry, Chicago, IL USA

Corresponding Author:
    Dingcai Cao, PhD
    Department of Ophthalmology and Visual Sciences
    University of Illinois at Chicago
    1905 W. Taylor Street, Room 149
    Chicago, IL 60615
    Tel: (312) 355-3662
    fax (312) 996-7770
    email: dcao98@uic.edu

Word counts: 4488

Abstract

Purpose: To evaluate contrast threshold and contrast gain in patients with optic neuritis under conditions designed to favor mediation by either the inferred Magnocellular (MC-) or Parvocellular (PC-) pathway.

Methods: Achromatic and chromatic contrast discrimination was measured in 11 patients with unilateral or bilateral optic neuritis and 18 age-matched controls with normal vision, using achromatic steady-pedestal and pulsed-pedestal paradigms to bias performance toward the MC- or PC- pathway respectively. Additionally, L-M chromatic discrimination at equiluminance was evaluated using the steady-pedestal paradigm. . A physiologically plausible model could describe the data with parameters accounting for contrast gain and contrast sensitivity in the inferred MC- or PC- pathway. The fitted parameters from the affected eye by optic neuritis were compared with those from the normal eyes using Generalized Estimation Equation (GEE) models that can account for within-subject correlations.

Results: Compared with normal eyes, the affected eyes had significantly higher saturation parameters when measured with both the achromatic pulsed-pedestal paradigm [GEE: β(se) = 0.35(0.06), p < 0.001] and the chromatic discrimination paradigm [β(se) = 0.18(0.08), p = 0.015], suggesting contrast gain in the inferred PC-pathway is reduced; the affected eyes also had reduced absolute sensitivity in the inferred MC-pathway measured with the achromatic steady-pedestal paradigm [β(se) = 0.12 (0.04), p = 0.005].

Conclusion: Optic neuritis produced large sensitivity loss mediated by the MC-pathway and contrast gain losses in the inferred PC- pathway. A clinical framework is presented for interpreting contrast sensitivity and gain loss to chromatic and achromatic stimuli in terms of retinal and post-retinogeniculate loci contributions to detection and discrimination.

Introduction

Optic neuritis refers to an inflammation of one or both optic nerves that is painful and results in temporary loss or blurring of vision. Vision typically recovers gradually when assessed with conventional clinical methods. Sensitive psychophysical approaches however, often reveal a long-lasting loss in spatial, temporal, luminance and/or chromatic visual function[1-15]. It is still to be determined how the reported luminance and chromatic sensitivity losses in optic neuritis reflect deficits in retinogeniculate and/or cortical function.

Modern anatomical and physiological studies have identified three major neural retinogeniculate pathways in the primate visual system that convey retinal information to visual cortex, the magnocellular (MC-), parvocellular (PC-) and koniocellular (KC-) pathways [16, 17]. These parallel pathways have distinctive temporal, spatial, chromatic and contrast response characteristics and mediate different aspects of vision [18, 19]. The MC-pathway sums signals from L- and M- cones [20-22], with receptive fields showing either on-center or off-center organization. The MC-pathway, because of its band-pass spatio-temporal characteristic with high temporal frequency sensitivity, is considered to have an important role in contrast detection over a wide range of luminances [23] and in providing input to higher order pattern and motion processes [24]. The PC-pathway, on the other hand, is considered to have primary roles in chromatic processing, visual acuity, and provides input to higher-order pattern processes [25]. In PC-pathway cells, spectral opponency to lights of varying spectral composition is obtained by differencing of L- and M- cone signals [20]. On- and off-center receptive field organization reveals four sub-types of PC-pathway cells. PC-pathway cells have a low-pass spatio-temporal

4

characteristic to chromatic stimuli and a band-pass spatio-temporal characteristic to achromatic stimuli. The achromatic temporal modulation transfer functions of PC-pathway cells show a lower cut-off frequency than do MC-pathway cells [26, 27]. The KC-pathway differences S-cone signals from the sum of the L- and M-cones, with the small bistratified ganglion cells [28] responding to increases in S-cone signal in the center or decreases in (L+M) in the surround. The KC-pathway, considered to underlie blue-yellow chromatic discrimination [29], is not evaluated in this study.

Typical clinical findings in optic neuritis include loss of visual acuity and color vision, two visual functions thought to be mediated by the PC- pathway [17]. The PC-pathway accounts for about 80% of optic nerve fibers [30], and there is considerable interest to determine if the visual deficit in optic neuritis occurs selectively in the thinly myelinated ganglion cells of the PC- pathway. Numerous attempts have been made to separate PC- and MC- mediated vision by taking advantage of different functional properties of the two pathways: the MC- pathway shows greater sensitivity to lower spatial frequencies, higher temporal frequencies, and achromatic targets; the PC-pathway shows greater sensitivity to higher spatial frequencies, lower temporal frequencies, and chromatic stimuli [3-15]. Typically, reduced chromatic or luminance sensitivity has been interpreted as PC- or MC- deficits, respectively, and it has been reported that the visual deficit in optic neuritis is greater in the PC- pathway than in the MC- pathway [9]. This interpretation is precarious since the PC-ganglion cell responds well to achromatic stimuli [18]. Further, different metrics used for achromatic and chromatic stimuli make the direct comparison of visual performance between the inferred PC- and MC- deficits difficult. Here we address two outstanding issues in the

5

study of luminance and chromatic sensitivity losses in optic neuritis using an experimental approach that measures the sensitivity of both pathways to the same spatio-temporal stimuli, a necessary requirement for interpreting the relative sensitivity losses in the two pathways. First, we determine achromatic contrast sensitivity in both the PC and MC pathways. Second, we determine PC-pathway achromatic and chromatic contrast gain response.

In this study, we investigated MC- and PC- deficits in optic neuritis using a set of psychophysical paradigms developed by Pokorny and Smith [31] to separate MC- and PC- pathway contrast discrimination based on differential contrast response characteristics of primate MC- and PC- cells. MC-cells show response saturation to luminance contrast while PC-cells response are relatively linear; and MC-cells have much greater contrast gain than PC-cells.[32] The PC chromatic contrast gain is intermediate between the achromatic MC and PC contrast gains.[33] Unlike stimulus paradigms used by previous studies, these paradigms measure the responses of the two pathways using identical stimuli that differ only in pre- and post-adaptation. We used two psychophysical paradigms: the *Pulsed-Pedestal* paradigm to reveal PC-contrast gain and the *Steady-Pedestal* paradigm to evaluate steady-state MC- pathway sensitivity. The rationale for the paradigms revealing MC- or PC- mediation are fully explained elsewhere.[31, 33-35] Briefly, PC- mediation of the pulsed-pedestal thresholds is inferred from the congruence of contrast gain parameters derived from the pulsed-pedestal data [31] and parameters from single unit primate retina PC recordings [32]. MC-mediation of the steady-pedestal thresholds is inferred from the similarity of contrast gain parameters derived from the pedestal-Δ-pedestal data and parameters from single

6

unit primate retina MC recordings. Although contrast gain is established in the retina, post-retinal factors can alter sensitivity and may modify contrast gain parameters [35]. The relative sensitivities of thresholds under the pulsed- and steady-pedestal paradigms are determined by the spatial and temporal presentation parameters. The stimulus parameters in the present experiment were chosen so as to obtain a large separation between inferred MC- and PC- function. Temporal summation data [31] and spatial summation data [36] show the optimal conditions for having the MC-pathway mediate steady-pedestal thresholds and the PC-pathway mediate pulsed-pedestal thresholds require briefly presented test stimuli (<50 ms) subtending about 1° visual angle.

This methodology has been adopted for use in a variety of clinical studies [34, 37-44]. Further, the chromatic contrast discrimination paradigm developed by Smith, Pokorny and Sun [45] extends the achromatic contrast discrimination tasks by evaluating chromatic contrast gain in the PC- pathway using the same spatial and adaptation configuration as for the achromatic paradigm. By this, we can evaluate the association between achromatic and chromatic contrast sensitivity and contrast gain in the PC-pathway and determine whether optic neuritis influences the association strength.

Methods

Apparatus and Calibration

The stimuli were displayed on a calibrated 17" NEC CRT color monitor controlled by a 10-bit Radius video card hosted in a Macintosh G4 computer. The CRT display was run at a refresh rate of 75 Hz to ensure artifacts generated by the raster scan would not affect discrimination threshold [46]. Calibration procedures have been described elsewhere [45].

Stimuli

A 2 x 2 pedestal array of four 1° squares (pedestal) separated by 0.06° was set within a uniform 9.2°x8.7° rectangular surround (Figure 1). For each trial, one square in the pedestal array was randomly chosen as the test square that differed in luminance or chromaticity from other squares during the stimulus presentation (4-alternative forced choice procedure). The pedestal was either pulsed simultaneously with the test square for 26.6 ms during the trial period (pulsed-pedestal condition) or presented continuously (the steady-pedestal condition). The stimulus configuration is therefore identical during the test period in the pulsed and steady paradigms. Figure 1 shows the stimulus configurations for the achromatic pulsed-pedestal, achromatic steady-pedestal and chromatic steady-pedestal conditions.

Throughout the experiment, the surround was metameric to the equal-energy-spectrum light [L/(L+M) = 0.665, S/(L+M) = 1.0]. The surround luminance was set to 12.0 cd/m^2 (115 effective Td in young normal adults [47]). It is possible that rods are active at this light level, however, rod contributions to the MC- or PC- pathway are very

weak for equal-energy-spectrum light stimuli at retinal illuminances higher than 100 Td [48, 49]. For luminance discrimination with the pulsed-pedestal and steady-pedestal conditions, there were five pedestal contrasts. The pedestal luminances were 7.6, 9.5, 12.0, 15.1 and 19.0 cd/m^2, respectively. For chromatic discrimination, there were five chromatic contrasts along the L/(L+M) axis with a constant S-cone excitation. The pedestal L/(L+M) chromaticities were 0.62, 0.64, 0.665, 0.68 and 0.70 respectively. For color normal observers, the chromatic steady and pulsed pedestal paradigms yield alike data.[45] Here we measured L/M discrimination threshold for the steady-pedestal condition only.

Observers

The sample included 18 control observers (14 females and 4 males) who had no health complaints, had their best corrected visual acuity of 20/20 or better, and had no history of eye disease and 11 observers with optic neuritis (9 females and 2 males). The normal observer and optic neuritis patient ages did not differ significantly [33.9(mean) $\pm$ 9.8(SD) vs. 38.2$\pm$10.7 years, p = 0.282]. Persons with optic neuritis were recruited from the patient population at the Illinois Eye Institute, Illinois College of Optometry, and the Eye Clinics of The University of Chicago. All observers (other than the investigators) were paid for their services. Patients were selected from a chart review to identify individuals with the following characteristics: Acute/subacute loss of vision in one or both eyes occurring over one week, improvement in vision beginning at four weeks after onset, often associated with loss of color vision and pain on eye movement, were between 18 and 60 years of age with no evidence of systemic

9

diseases associated with optic neuritis or other eye disease. All patients had a comprehensive ophthalmological examination. The episode of optic neuritis occurred at least six months prior to inclusion and the best corrected visual acuity at the time of entry was better than 20/50. The characteristics of the 11 optic neuritis patients are listed in Table 1. Among the patients, eight had bilateral optic neuritis and three had unilateral optic neuritis. Seven patients were diagnosed with multiple sclerosis (MS), two (P6 and P9) did not have MS, while a diagnosis of MS was indeterminable in two patients (P1 and P10).

Procedure

During experiments, the observer sat in a dimly lit room at 1 m away from the display. The observer monocularly viewed the stimuli. A black eye patch covered the non-tested eye. Prior to each session, the observer dark-adapted for 3 minutes. Each condition began with a 2-minute adaptation period to the surround light level to stabilize the observer's adaptation. For the steady-pedestal paradigm, there was an additional 1-minute period of adaptation to the pedestal and surround. Short auditory beeps signaled the beginning and end of each adaptation period, and the start of each trial. A fixation square (4' arc), present between trials to aid fixation, extinguished to signal the trial onset. A random-double staircase procedure was used to determine a discrimination threshold. In one staircase, the test square threshold was measured in an increment direction, in the other, a decrement direction. During each trial, the observer's task was to identify the location of the test square within the 4 square pedestal array by moving the mouse cursor into the area where the test square

appeared. No feedback was provided. Ten reversals were measured for both the

increment and the decrement staircases. The average of the last six reversals was

taken as threshold. Including short breaks, the total test time for all three conditions

with one eye was about 45 minutes. Once one eye was tested, the observer could

choose to test the other eye after an extended break or on another day.

Modeling

The luminance and chromatic discrimination data are presented in the results as

the change in L-cone cd/m^2 (ΔL) as a function of pedestal L-cone cd/m^2. Note the L-

cone cd/m^2 is equivalent to 0.665 of the luminance value for luminance discrimination

data, which were fitted by a physiological based contrast response model for MC- and

PC- pathways [31, 33]. The achromatic contrast response is described by a Michaelis-

Menten saturation function [32]:

$$R = R_0 + R_{max}\ C/(C_{sat} + C) \tag{1},$$

where R_{max} is the maximum response rate, C_{sat} is the half-maximum contrast response

and C is the stimulus Michelson contrast. Contrast gain is defined as R_{max}/C_{sat}, the

derivative of Equation 1 at zero contrast (C = 0). Therefore, contrast gain expressed in

logarithmic units is linearly related to -log(C_{sat}). A contrast discrimination threshold can

be obtained when the differential responses to two contrasts [C and a (C+ΔC)] reaches

the criterion, δ. Therefore, the pulsed-pedestal luminance discrimination threshold can

be derived from equation (1):

$$\log(\Delta L) = K_{p\_a} + \log[(C + C_{sat\_a})^2] - \log[C_{sat\_a} - k(C + C_{sat\_a})] \tag{2}$$

11

where ΔL is discrimination threshold in L-cone cd/m^2, K_{p_a} ("p" denotes pulsed, "a" denotes achromatic) is the vertical scaling parameter in logarithmic unit that represents PC-mediated absolute threshold (therefore - K_{p_a} represents contrast sensitivity), and k represents (δ/R_{max}), which is typically small and was set as zero when fitting the pulsed-pedestal data. There are two free parameters for the achromatic pulsed-pedestal condition (K_{p_a} and C_{sat_a}). Note that the zero contrast data were not used for pulsed-pedestal model fitting because the pulsed- and steady-pedestal conditions have the same (zero contrast) stimulus and detection was empirically established to be mediated by the inferred MC-pathway. The steady-pedestal luminance discrimination data for a pedestal luminance, L (in L-cone cd/m^2), are described by

$$\log(\Delta L) = K_{s\_a} + \log(L) \tag{3},$$

where Ks_a is the vertical scaling parameter in logarithmic units that represents absolute threshold in logarithmic units. Therefore, -Ks_a represents MC-mediated absolute sensitivity.

The L/M chromatic discrimination data were fitted with a model of L and M cone spectral processing based on the spectral opponent PC pathway of primates [20, 26, 50]. Briefly, following a gain control mechanism of L and M cone excitations, the spectral opponent signal is subject to subtractive feedback. The response to a chromatic contrast change from the adapting chromaticity then follows a static saturation function describing retinal ganglion PC cell responses to contrast changes from their adapted steady-state level. The details of the chromatic discrimination model are described elsewhere [45, 51]. The L/M chromatic discrimination data were fitted with the model:

$$\log(\Delta L) = K_{s\_c} + \log[(\Delta OPP + OPP_A + SAT_c)^2/SAT] - \log[l_{max}/G(L) + m_{max}/G(M)]$$

(4)

where K_{s_c} ("s" denotes steady, "c" denotes chromatic) represents the vertical scaling factor expressed in logarithmic units (therefore, $-K_{s\_c}$ for contrast sensitivity), OPP_A represents the spectral response to the adapting chromaticity ΔOPP represents the change in the spectral response with the pedestal chromaticity from the adapting chromaticity, and SAT_c is the PC- spectral processing half-saturation term. Note the saturation term (SAT_c) does not have the same meaning as that for achromatic discrimination (C_{sat_a}). For achromatic discrimination, C_{sat_a} is in the physical contrast domain, while SAT_c is in the spectral response domain. There are two free parameters for the L/M chromatic discrimination model ($K_{s\_}$ and SAT_c).

Statistical Analysis

Three of the patients had unilateral defects based on the clinical criteria defined in the Methods section. The unaffected eyes of the patients were excluded from analysis. Each observer's fitted luminance and chromatic model parameters were used for further statistical analysis. First, we examined the distributions of the parameters. Some of the parameters were not normally distributed. Although a non-parametric approach might be appropriate for analysis because there would be no requirement for normality, it has limitations in controlling confounding factors such as age, or dealing with correlations between the eyes of the observers. We preferred to rely on parametric methods to compare the fitted model parameters between affected and non-affected eyes and a log transform proved satisfactory to establish normality. To examine the

13

functional loss of optic neuritis, a Generalized Estimation Equation (GEE) modeling

approach was used to account for correlations between two eyes from the same

observer[52]. GEE analysis is a modern version of repeated measures ANOVA with

flexibility for fitting outcome variables with various distributions by application of link

functions and specifying the variance-covariance structure in repeated measurements

using a "sandwich" algorithm. We used an identity link function for the fitted parameters

that were considered to have normal distributions. The GEE models compared the

parameters between affected eyes (coded as 1) and normal eyes (coded as 0). For all

of the GEE analyses, age was controlled because aging is an important factor for MC-

and PC- mediated detection or discrimination[37]. Since not all of the optic neuritis were

identified as caused by MS, we conducted additional GEE analysis with MS patients

only. GEE models were used to assess the association between two fitted model

parameters and whether the strength association differed between normal observers

and optic neuritis patients, with one parameter as the outcome. The independent

variables included the other parameter, disease group (affected, coded as 1, vs. normal,

coded as 0) and their interaction. A significant interaction would indicate the association

strength differs between the groups. When the association between achromatic steady

and pulsed paradigms was assessed, the parameters from the pulsed paradigm were

used as the outcome variables; when the association between the steady chromatic

paradigm and the achromatic pulsed paradigm was evaluated, the parameters from the

chromatic paradigm were the outcome variables. When the association between the

gain parameter and absolute sensitivity parameter was assessed, the gain parameter

was the outcome variable.

Results

First, we investigated the functional loss in optic neuritis by comparing the estimated

parameters between the normal observers and optic neuritis patients. Then we

evaluated how the estimated parameters related to each other in the normal observers

or patients.

Functional loss in optic neuritis

We estimated the 95% confidence intervals for the luminance and chromatic

discrimination thresholds for each paradigm as a function of pedestal L-cone cd/m^2 for

the normal observers from their model parameters (Eqs. 2-4). The luminance and

chromatic discrimination thresholds of each participant with optic neuritis are plotted in

reference to the 95% confidence intervals of the normal observers (grey shaded bands

in Figures 2 and 3).

Figure 2 shows the individual optic neuritis patient's luminance discrimination for

the pulsed-pedestal (unfilled symbols) and steady-pedestal (filled symbols) conditions

and the best-fitting models (lines). Thirteen out of the 19 optic neuritis eyes had

discrimination data falling outside of the 95% confidence interval of the controls. There

is evidence for differential sensitivity losses in MC- and PC- contrast sensitivity and for

changes in the slopes of the PC contrast discrimination function in optic neuritis eyes.

Figure 3 shows the individual optic neuritis patients' chromatic discrimination data. Ten

out of 19 optic neuritis eyes had chromatic contrast discrimination functions that differed

in either shape or sensitivity compared to the control limits. The differential effect of

optic neuritis on PC mediated achromatic and chromatic contrast discrimination will be considered next.

To directly evaluate the change in contrast sensitivity to achromatic (inferred MC- and PC-) and chromatic (inferred PC-) stimuli, and the contrast gain of the PC- pathway to achromatic and chromatic stimuli in patients with optic neuritis, we analyzed the parameters from the physiologically based model. It was first determined by inspection of the distributions of the fitted parameters that there were no major deviations from a normal distribution for Kp_a, Ks_a, and Ks_c. The parameter Csat_a and SATc were not normally distributed and log transformations, which are directly related to log contrast gain [-log(Csat_a) or -log(Csat_c) for contrast gains], satisfied normal distribution criteria and were used for GEE analysis. Figure 4 shows the fitted contrast sensitivities (-Ks_a, -Kp_a, and -Kp_c) and contrast gains [-log(Csat_a) or -log(Csat_c)] in normal eyes and affected eyes in optic neuritis patients. The affected eyes had significantly higher Ks_a than normal eyes [β(se) = 0.12 (0.04), p = 0.005], suggesting optic neuritis. The affected eyes also had higher log(Csat_a) [β(se) = 0.35(0.06), p < 0.001] and higher log(SATc) [β(se) = 0.18(0.08), p = 0.015], suggesting optic neuritis reduced PC-mediated contrast gain for achromatic and chromatic processing. However, Kp_a and Ks_c were not significantly different between normal eyes and affected eyes [Kp_a: β(se) = -0.03(0.04), p = 0.461; Ks_c: β(se) = 0.53(0.46), p = 0.255], indicating optic neuritis did not significantly affect PC-mediated detection sensitivity. Additional analysis with the subset of seven patients with MS revealed the same results. That is, the affected eyes in MS patients had reduced MC-mediated absolute sensitivity (p < 0.001) and PC-mediated contrast gain estimated from the

16

achromatic pulsed pedestal paradigm (p < 0.001) and chromatic steady pedestal paradigm (p = 0.049), but did not alter PC-mediated detection sensitivity (p = 0.628 for achromatic pulsed pedestal paradigm and p =0.121 for chromatic steady pedestal paradigm).

Association among fitted parameters for the PC-pathway

GEE modeling showed that the association strength did not differ between normal observers and optic neuritis patients, as none of the interaction terms between disease and the model parameter that served as the independent variables was significant (ps ≥ 0.201). For the achromatic pulsed-paradigm and the chromatic steady-paradigm, both mediated by the PC-pathway, the vertical scaling parameters were highly associated [K_{s_c} vs. K_{p_a}: β(se) = 0.14(0.04), p < 0.001], indicating a common mechanism determined these values. However, the logarithmic saturation parameters were not significantly associated [log($SAT_{\_c}$) vs. log(C_{sat_a}): β(se) = 0.14(0.18), p = 0.431], consistent with physiological findings that PC- cell responses have higher contrast gain with chromatic stimuli than achromatic stimuli and PC chromatic responses may be saturated with a high chromatic contrast [18]. Further, the sensitivity parameter was associated with the logarithmic saturation parameter for the achromatic paradigm [log(C_{sat_a}) vs. K_{p_a}: β(se) = -0.71(0.29), p = 0.014]. For the chromatic paradigm, the logarithmic saturation parameter and sensitivity parameter were not associated in both observer groups [log($SAT_{\_c}$) vs. K_{s_c}: β(se) = -0.79(1.19), p = 0.510; disease x K_{s_c} interaction: β(se) = -1.46(2.00), p = 0.465], suggesting that factors in addition to contrast gain contribute to sensitivity in PC-pathway chromatic processing.

Discussion

The comparison between normal observers and optic neuritis patients in achromatic and chromatic discrimination suggests the eyes affected by optic neuritis suffered deficits in both the inferred MC- and PC- pathways, but in different ways. Specifically, optic neuritis reduced MC-mediated absolute sensitivity but reduced PC-mediated contrast gain. Interestingly, the disease did affect the association strength among PC-mediated contrast sensitivities and contrast gains measured from achromatic and chromatic stimuli. Our results imply that for that MC-pathway contrast sensitivity suffered a larger loss. However, we could not compare relative loss in contrast gain between the two pathways since we did not measure MC-mediated contrast gain.

In this study, the contrast discrimination and detection thresholds (Figure 2 and 3) are modeled within a perceptual-decision framework [31, 33, 34]. That is, a decision ("different or same" for discrimination, "seeing it or not" for detection) will be made once the sensory input reaches a criterion value (i.e. the comparison of sensory input and the criterion). Sensory input is determined by retinal processing, from photoreceptor transduction to ganglion cell contrast responses transmitted via the optic nerve. Perceptual-decision processing is determined in the cortex. In normal observers, the signature V-shape of the contrast discrimination and detection functions (Figures 2 and 3) is defined at a retinal site, principally at the bipolar cell level [35]. Disease alters the contrast gain and sensitivity of the measured contrast discrimination functions by changing neuronal function at one or multiple sites in the visual pathway [35]. Simply, contrast gain and sensitivity can be considered within this framework at three sites: a

18

site prior to the contrast-processing site (outer retina, photoreceptor level), within the site that defines the signature V-shape (inner retina, bipolar or ganglion cells), or at post-retinal sites (optic nerve, cortex).

An alteration in contrast sensitivity in the presence of normal contrast gain can result from a change in quantum efficiency and/or phototransduction noise in the photoreceptors, or a change in decision processing (such as decision criterion variation or a change in sensory information accumulation) [35] in the cortex. At the photoreceptor level, a decrease in quantum efficiency or noise can lead to a change in contrast sensitivity in the pedestal tasks, but even a 10-time decrease (1 log unit) in photopic light level does not reduce cone contrast gain substantially for estimated PC- [53] or MC-pathways [54, 55]. The functional consequences of early changes are complex and not easy to characterize because of the compensatory effects of retinal adaptational mechanisms.   Studies show that stimulus noise can decrease chromatic sensitivity without altering contrast gain parameters [56] and adding noise to the stimuli may differentially impact on PC- and MC- contrast sensitivity [57]. Therefore, the reduction in MC-mediated contrast sensitivity in the optic neuritis patients observed in this study may reflect an anomalous retinal and/or higher-order processing. It has been previously recognized that if LGN inputs to the cortex are impaired, there may be adaptive changes in the cortex, such as lateral occipital complexes and other higher visual areas, possibly leading to a change in decision processing [58-60].

A change in contrast gain alters the slopes of the V-shaped contrast discrimination function and can be caused by an alteration in neural noise (arising in the retinal contrast-processing site, post-retinal site, including optic nerve or cortex), or

response compression (from a retinal or post-retinal site) [35]. Noise arising in the optic

nerve or brain can also change the contrast gain. One way of characterizing the

precision of information carried in a spike train is by the signal-to-noise ratio.

Recordings from cat X- and Y- [61] and primate PC- and MC-ganglion cells [62] show noise

to be relatively independent of contrast. Since stimulus related spike rate increases

with contrast, the signal-to-noise ratio increases with contrast. If there is sufficient post-

retinal noise to degrade visual function, the measured contrast gain function will be

altered in a specific way. The signal-to-noise ratio for a discrimination near the adapting

retinal illuminance will be lower than signal-to-noise ratio for a discrimination that

involves a large step from the adapting retinal illuminance. Thus the arms of the V will

assume shallower slopes. Observers would require more contrast to discriminate

contrast changes at low pedestal contrasts compared to higher pedestal contrasts,

indicative of a specific type of shallowing of the contrast gain slope. Response

compression, however, will produce a different alteration in the contrast gain function.

With large contrast steps from the adapting retinal illuminance, a higher than normal

contrast is required for discrimination. Thus discrimination near the adapting retinal

illuminance could be normal or near normal whereas discrimination for a stimulus with a

large contrast step from the adapting retinal illuminance could be impaired. We saw V-

shapes from optic neuritis data that were consistent with either the neural noise

interpretation (e.g. P9, OD, Fig. 2) or the response compression interpretation (e.g. P3,

OD, Fig. 2). This analysis suggested that PC-mediated contrast gain loss had multiple

etiologies, some might be retinal and some might be post-retinal.

As we know from optical coherence tomography (OCT) analysis, retinal nerve fiber layer (RNFL) attenuation can occur in patients with MS who have never suffered an episode of optic neuritis.[63] That said, those individuals with an established history of optic neuritis typically have significantly more NFL attenuation as compared to MS without optic neuritis [64, 65]. The OCT results we have for three patients (5/6 eyes affected) in this study (P2, P9, P11), showed a reduction in RNFL thickness in 5 affected eyes [74(mean)±6.2µm(SD)], compared with normative data. RNFL thicknesses and contrast sensitivity and gain parameters were all negatively correlated, though not reaching statistical significance due to a small sample size (Pearson correlation between -0.31 and -0.83, ps = 0.08-0.61). These results implicate alterations in retinal processing playing a significant role in reducing MC-mediated sensitivity and PC-mediated contrast gain in patients with optic neuritis, though we cannot rule out the involvement of alterations in higher-order processing.

Acknowledgement

References

1.   Hess RF, Plant GT. The psychophysical loss in optic neuritis: Spatial and temporal aspects. In: Hess RF, Plant GT (eds), *Optic Neuritis.* Cambridge: University of Cambridge Press; 1986:109-151.

2.   Foster DH. The psychophysical loss in optic neuritis: Luminance and colour aspects. In: Hess RF, Plant GT (eds), *Optic Neuritis.* Cambridge: University of Cambridge Press; 1986:152-191.

3.   Rucker JC, Sheliga BM, FitzGibbon EJ, Miles FA, Leigh RJ. Contrast sensitivity, first-order motion and initial ocular following in demyelinating optic neuropathy. *J Neurol* 2006;253:1203-1209.

4.   Caruana PA, Davies MB, Weatherby SJM, et al. Correlation of MRI lesions with visual psychophysical deficit in secondary progressive multiple sclerosis. *Brain* 2000;123:1471-1480.

5.   Fallowfield L, Krauskopf J. Selective loss of chromatic sensitivity in demyelinating disease. *Investigative Ophthalmology & Visual Science* 1984;25:771.

6.   Flanagan P, Zele AJ. Chromatic and luminance losses with multiple sclerosis and optic neuritis measured using dynamic random luminance contrast noise. *Ophthalmic Physiol Opt* 2004;24:225-233.

7.   Flanagan P, Markulev C. Spatio-temporal selectivity of loss of colour and luminance contrast sensitivity with multiple sclerosis and optic neuritis. *Ophthalmic Physiol Opt* 2005;25:57-65.

8.   Grigsby SS, Vingrys AJ, Benes SC, Kingsmith PE. Correlation of Chromatic,

Spatial, and Temporal Sensitivity in Optic-Nerve Disease. *Investigative Ophthalmology*

& Visual Science 1991;32:3252-3262.

9.   Porciatti V, Sartucci F. Retinal and cortical evoked responses to chromatic

contrast stimuli - Specific losses in both eyes of patients with multiple sclerosis and

unilateral optic neuritis. *Brain* 1996;119:723-740.

10.   Mullen KT, Plant GT. Color and Luminance Vision in Human Optic Neuritis. *Brain*

1986;109:1-13.

11.   Moura ALD, Teixeira RAA, Oiwa NN, et al. Chromatic discrimination losses in

multiple sclerosis patients with and without optic neuritis using the Cambridge Colour

Test. *Vis Neurosci* 2008;25:463-468.

12.   Mullen KT, Plant GT. Anomalies in the Appearance of Colors and of Hue

Discrimination in Optic Neuritis. *Clin Vision Sci* 1987;1:303-316.

13.   Plant GT, Hess RF. Temporal Frequency Discrimination in Optic Neuritis and

Multiple-Sclerosis. *Brain* 1985;108:647-676.

14.   Dain SJ, Rammohan KW, Benes SC, Kingsmith PE. Chromatic, Spatial, and

Temporal Losses of Sensitivity in Multiple-Sclerosis. *Investigative Ophthalmology &*

Visual Science 1990;31:548-558.

15.   Ventura DF, Quiros P, Carelli V, et al. Chromatic and luminance contrast

sensitivities in asymptomatic carriers from a large Brazilian pedigree of 11778 Leber

hereditary optic neuropathy. *Investigative Ophthalmology & Visual Science*

2005;46:4809-4814.

16.   Dacey DM. Parallel pathways for spectral coding in primate retina. *Annu Rev Neurosci* 2000;23:743-775.

17.   Kaplan E. The M, P, and K Pathways of the Primate Visual System. In: Chalupa LM, Werner JS (eds), *The Visual Neuroscience.* Cambridge, MA: MIT Press; 2004:481-493.

18.   Lee BB, Martin PR, Valberg A. Sensitivity of macaque retinal ganglion cells to chromatic and luminance flicker. *Journal of Physiology (London)* 1989;414:223-243.

19.   Kaplan E, Lee BB, Shapley RM. New views of primate retinal function. In: Osborne N, Chader J (eds), *Progress in Retinal Research.* Oxford: Pergamon press; 1990:273-336.

20.   Derrington AM, Krauskopf J, Lennie P. Chromatic mechanisms in lateral geniculate nucleus of macaque. *Journal of Physiology (London)* 1984;357:241-265.

21.   Shapley RM, Reid RC, Kaplan E. Receptive field structure of P and M cells of the monkey retina. In: Valberg A, Lee BB (eds), *From Pigments to Perception; Advances in Understanding the Visual Process.* New York: Plenum Press; 1991:95-104.

22.   Smith VC, Lee BB, Pokorny J, Martin PR, Valberg A. Responses of macaque ganglion cells to the relative phase of heterochromatically modulated lights. *Journal of Physiology (London)* 1992;458:191-221.

23.   Shapley RM, Enroth-Cugell C. Visual adaptation and retinal gain controls. *Prog Retin Eye Res* 1984;3:263-346.

24.   Ferrera VP, Nealey TA, Maunsell JH. Mixed parvocellular and magnocellular geniculate signals in visual area V4. *Nature* 1992;358:756-761.

25.   Lennie P. Roles of M and P Pathways. In: Shapley R, Lam DMK (eds), *Contrast Sensitivity.* Cambridge MA: MIT Press; 1993:201-213.

26.   Lee BB, Pokorny J, Smith VC, Martin PR, Valberg A. Luminance and chromatic modulation sensitivity of macaque ganglion cells and human observers. *Journal of the Optical Society of America A* 1990;7:2223-2236.

27.   Purpura K, Tranchina D, Kaplan E, Shapley RM. Light adaptation in the primate retina: analysis of changes in gain and dynamics of monkey retinal ganglion cells. *Vis Neurosci* 1990;4:75-93.

28.   Dacey DM, Lee BB. The 'blue-on' opponent pathway in primate retina originates from a distinct bistratified ganglion cell type. *Nature* 1994;367:731-735.

29.   Pokorny J, Smith VC. Chromatic Discrimination. In: Chalupa LM, Werner JS (eds), *The Visual Neuroscience.* Cambridge, MA: MIT Press; 2004:908-923.

30.   Shapley R. Visual sensitivity and parallel retinocortical channels. *Annu Rev Psychol* 1990;41:635-658.

31.   Pokorny J, Smith VC. Psychophysical signatures associated with magnocellular and parvocellular pathway contrast gain. *Journal of the Optical Society of America A* 1997;14:2477-2486.

32.   Kaplan E, Shapley RM. The primate retina contains two types of ganglion cells, with high and low contrast sensitivity. *Proc Natl Acad Sci U S A* 1986;83:2755-2757.

33.   Smith VC, Pokorny J. Psychophysical correlates of Parvo- and Magnocellular function. In: Mollon J, Pokorny J, Knoblauch K (eds), *Normal and defective colour vision*: Oxford University Press; 2003:91-107.

34.   Zele AJ, Wood JM, Girgenti CC. Magnocellular and parvocellular pathway mediated luminance contrast discrimination in amblyopia. *Vision Res* 2010;50:969-976.

35.   Pokorny J. Review: Steady and pulsed pedestals, the how and why of postreceptoral pathway separation. *J Vis* 2011;11(5):7:1-23.

36.   Smith VC, Sun VC, Pokorny J. Pulse and steady-pedestal contrast discrimination: effect of spatial parameters. *Vision Res* 2001;41:2079-2088.

37.   Elliott SL, Werner JS. Age-related changes in contrast gain related to the M and P pathways. *J Vis* 2010;10:4: 1-15.

38.   Alexander KR, Pokorny J, Smith VC, Fishman GA, Barnes CS. Contrast discrimination deficits in retinitis pigmentosa are greater for stimuli that favor the magnocellular pathway. *Vision Res* 2001;41:671-683.

39.   Alexander KR, Barnes CS, Fishman GA. Characteristics of contrast processing deficits in X-linked retinoschisis. *Vision Res* 2005;45:2095-2107.

40.   Sun H, Swanson WH, Arvidson B, Dul MW. Assessment of contrast gain signature in inferred magnocellular and parvocellular pathways in patients with glaucoma. *Vision Res* 2008;48:2633-2641.

41.   McKendrick AM, Badcock DK, Morgan WH. Psychophysical measurement of neural adaptation abnormalities in magnocellular and parvocellular pathways in glaucoma. *Investigative Ophthalmology & Visual Science* 2004;45:1846-1853.

42.   Battista J, Badcock DR, McKendrick AM. Spatial Summation Properties for Magnocellular and Parvocellular Pathways in Glaucoma. *Investigative Ophthalmology & Visual Science* 2009;50:1221-1226.

43.   Gualtieri M, Bandeira M, Hamer RD, et al. Psychophysical analysis of contrast processing segregated into magnocellular and parvocellular systems in asymptomatic carriers of 11778 Leber's hereditary optic neuropathy. *Vis Neurosci* 2008;25:469-474.

44.   McKendrick AM, Badcock DR. Constrast-processing dysfunction in both magnocellular and parvocellular pathways in migraineurs with or without aura. *Investigative Ophthalmology & Visual Science* 2003;44:442-448.

45.   Smith VC, Pokorny J, Sun H. Chromatic contrast discrimination: Data and prediction for stimuli varying in L and M cone excitation. *Color Res Appl* 2000;25:105-115.

46.   Zele AJ, Vingrys AJ. Cathode-ray-tube monitor artefacts in neurophysiology. *J Neurosci Methods* 2005;1-7.

47.   Le Grand Y. Light, Colour and Vision. Second Edition. London: Chapman and Hall; 1968:1-564.

48.   Cao D, Pokorny J, Smith VC. Matching rod percepts with cone stimuli. *Vision Res* 2005;45:2119-2128.

49.   Cao D, Pokorny J, Smith VC, Zele AJ. Rod contributions to color perception: Linear with rod contrast. *Vision Res* 2008;48:2586-2592.

50.   Lee BB, Pokorny J, Smith VC, Kremers J. Responses to pulses and sinusoids in macaque ganglion cells. *Vision Res* 1994;34:3081-3096.

51.   Zele AJ, Smith VC, Pokorny J. Spatial and temporal chromatic contrast: Effect on chromatic contrast discrimination for stimuli varying in L- and M-cone excitation. *Vis Neurosci* 2006;23:495-501.

52.   Liang KY, Zeger SL. Longitudinal Data-Analysis Using Generalized Linear-Models. *Biometrika* 1986;73:13-22.

53.   Sun H, Smith VC, Pokorny J. Decreasing surround size fails to alter chromatic discrimination. *Investigative Ophthalmology & Visual Science Supplement* 1998;39:S162.

54.   Cao D, Pokorny J. Rod and cone contrast gains derived from reaction time distribution modeling. *J Vis* 2010;10:11, 11-15.

55.   Cao D, Lee BB, Sun H. Combination of rod and cone inputs to in the parasol ganglion cells of the magnocellular pathway *J Vis* 2010;10:4, 1-15.

56.   Watanabe A, Pokorny J, Smith VC. Red-green chromatic discrimination with variegated and homogeneous stimuli. *Vision Res* 1998;38:3271-3274.

57.   McAnany JJ, Alexander KR. Spatial contrast sensitivity in dynamic and static additive luminance noise. *Vision Res* 2010.

58.   Faro SH, Mohamed FB, Tracy JI, et al. Quantitative functional MR imaging of the visual cortex at 1.5 T as a function of luminance contrast in healthy volunteers and patients with multiple sclerosis. *American journal of neuroradiology* 2002;23:59-65.

59.   Korsholm K, Madsen KH, Frederiksen JL, Skimminge A, Lund TE. Recovery from optic neuritis: an ROI-based analysis of LGN and visual cortical areas. *Brain* 2007;130:1244-1253.

60.   Levin N, Orlov T, Dotan S, Zohary E. Normal and abnormal fMRI activation patterns in the visual cortex after recovery from optic neuritis. *Neuroimage* 2006;33:1161-1168.

61.   Passaglia CL, Troy JB. Information transmission rates of cat retinal ganglion cells. *J Neurophysiol* 2004;91:1217-1229.

62.   Croner LJ, Purpura K, Kaplan E. Response variability in retinal ganglion cells of primates. *Proc Natl Acad Sci U S A* 1993;90:8128-8130.

63.   Fisher JB, Jacobs DA, Markowitz CE, et al. Relation of visual function to retinal nerve fiber layer thickness in multiple sclerosis. *Ophthalmology* 2006;113:324-332.

64.   Trip SA, Schlottmann PG, Jones SJ, et al. Optic nerve atrophy and retinal nerve fibre layer thinning following optic neuritis: evidence that axonal loss is a substrate of MRI-detected atrophy. *Neuroimage* 2006;31:286-293.

65.   Trip SA, Schlottmann PG, Jones SJ, et al. Retinal nerve fiber layer axonal loss and visual dysfunction in optic neuritis. *Ann Neurol* 2005;58:383-391.

Figure Captions

Figure 1: Stimulus paradigms for the achromatic pulsed-pedestal condition (top panel), achromatic steady-pedestal condition (middle panel), and chromatic steady-pedestal condition (bottom panel). All three paradigms shared the same spatial stimulus configuration. A pedestal consisting of a 2 x 2 pedestal array of four 1° squares separated by 0.06° was set within a uniform 9.2°x8.7° rectangular surround. For each trial, one square in the pedestal array was randomly chosen as the test square that differed in luminance or chromaticity from other squares during the stimulus presentation. The observer's task was to identify which square differed from the other three. The pedestal was either pulsed simultaneously with the test square for 26.6 ms during the trial period (pulsed-pedestal condition) or presented continuously (the steady-pedestal condition). The achromatic pulsed-pedestal condition reveals PC-pathway achromatic contrast gain, the achromatic steady-pedestal condition reveals steady state MC-pathway sensitivity, and the chromatic steady-pedestal condition reveals PC-pathway chromatic contrast gain.

Figure 2: The luminance discrimination threshold for optic neuritis patients, in reference of the 95% confidence intervals (the shaded grey area) defined by the normal observer data. Open symbols show data for the achromatic pulsed-pedestal paradigm (open red squares for right eyes, OD and open green circles for left eyes, OS); solid symbols show data for the achromatic steady-pedestal paradigm (solid red squares for right eyes, OD and solid green circles for left eyes, OS). The lines are model fits of Eqs. (2) and (3). An arrow shows the retinal illuminance of the surround.

Figure 3: The L/M discrimination threshold for optic neuritis patients, in reference of the 95% confidence intervals (the shaded grey area) defined by the normal observer data. Solid red squares show data for right eyes, OD, and solid green circles show data for left eyes, OS. The lines are model fits of Eq. (4). An arrow shows the retinal illuminance of the surround.

Figure 4: Box plots for the median (50th percentile, the band inside the box) and interquartile range (25th–75th percentile, the bottom and top of the box) of the fitted contrast sensitivity and contrast gain parameters in normal eyes and affected eyes. Left column shows model parameters for achromatic paradigms (top panel for steady-pedestal, middle and bottom panels for pulsed-pedestal). Right column shows model parameters for chromatic paradigm. The p-values were resulted from age-controlled GEE analyses.
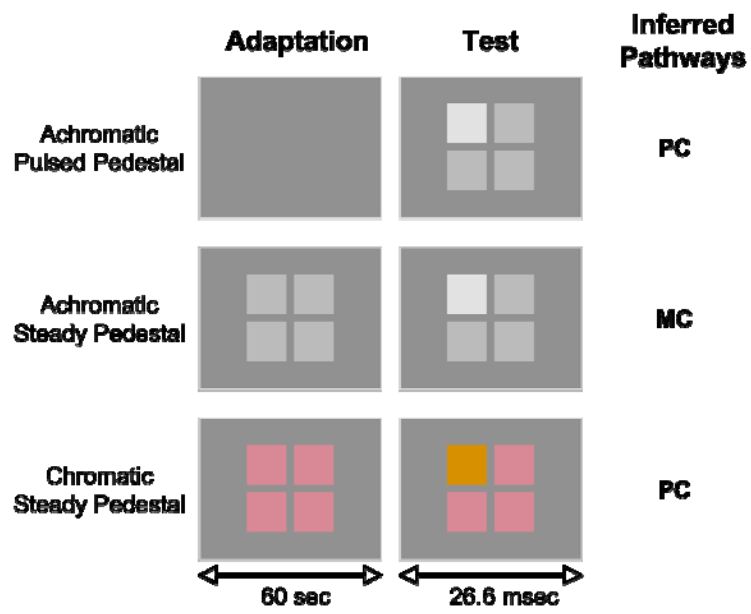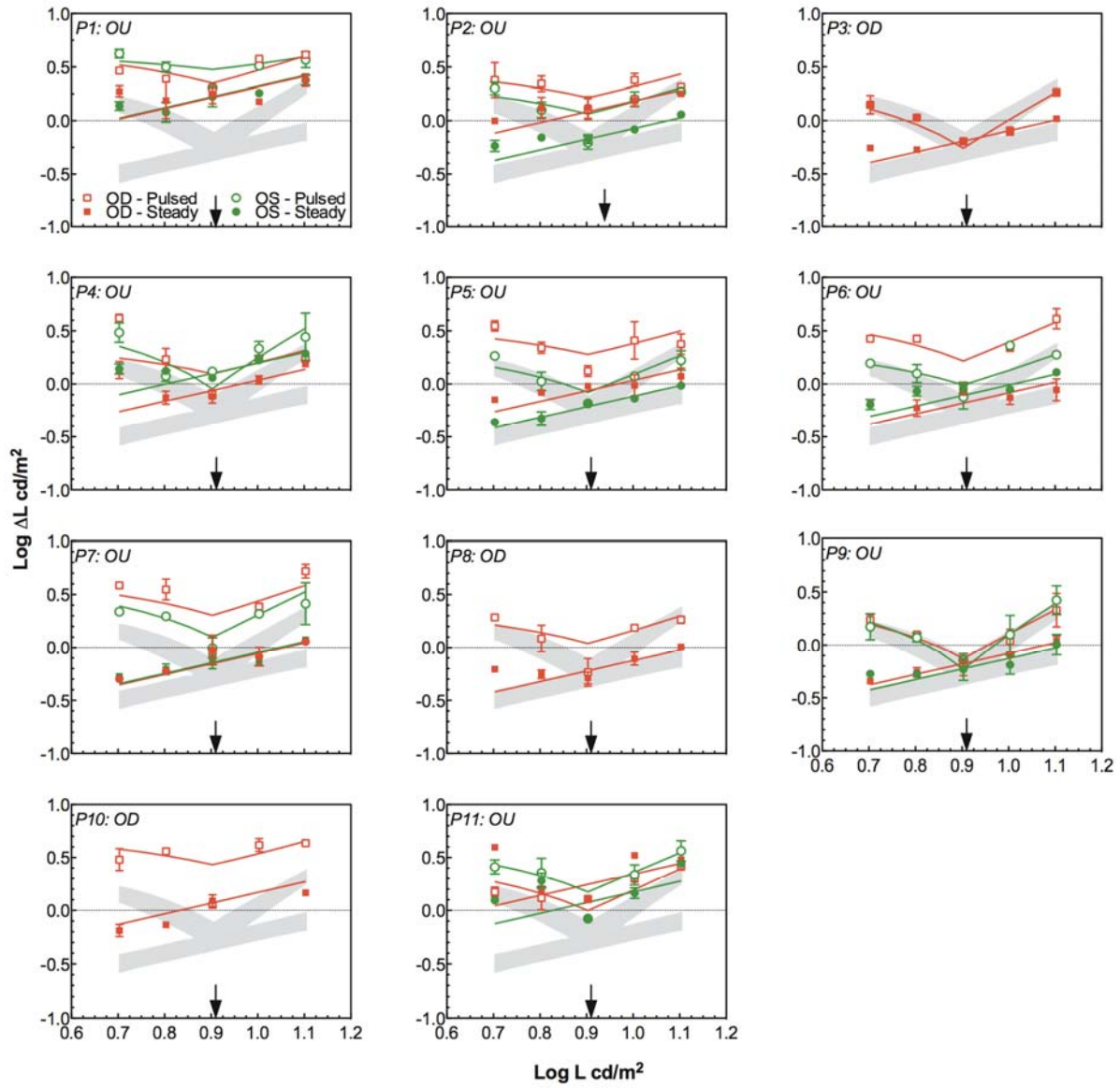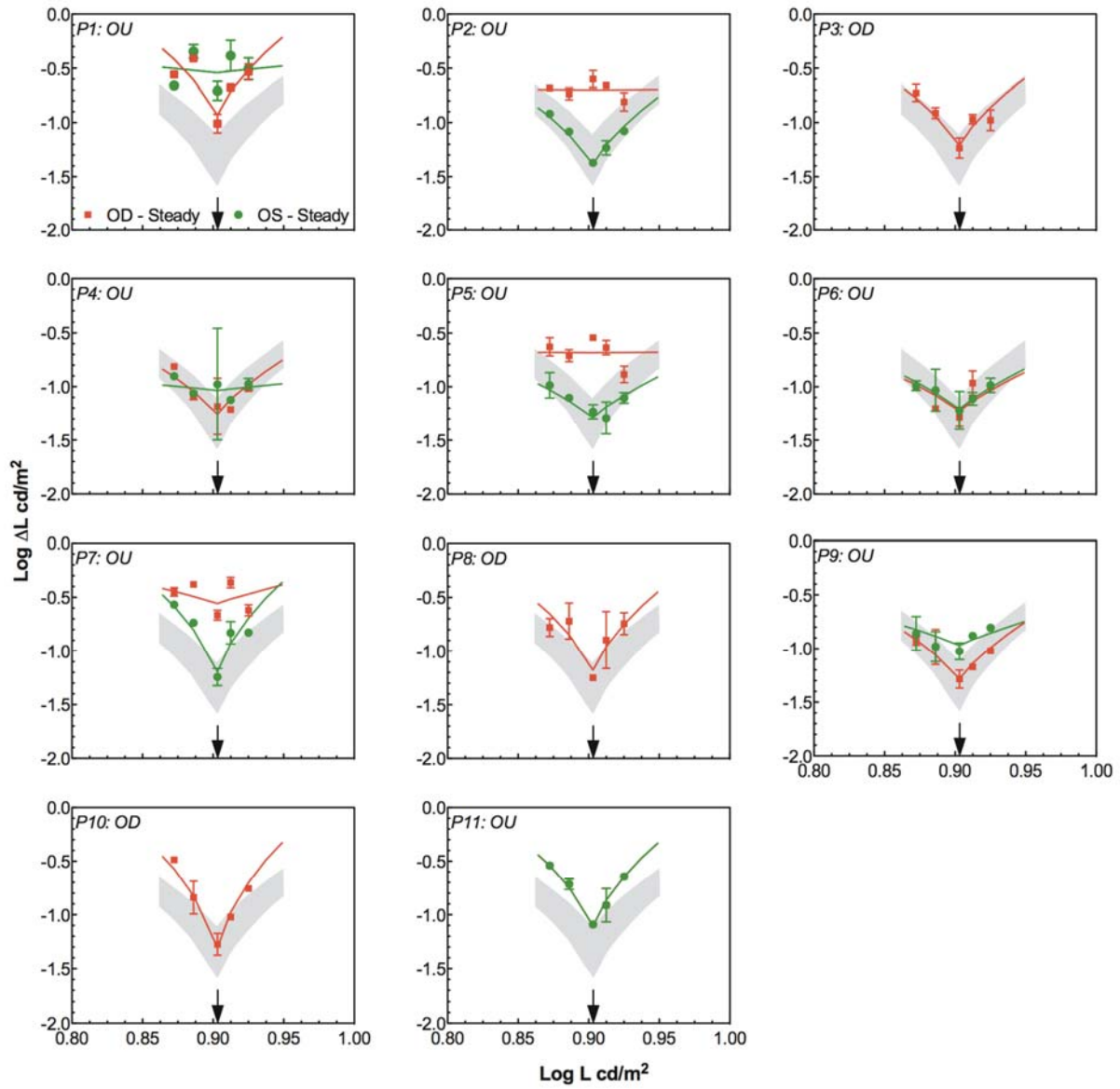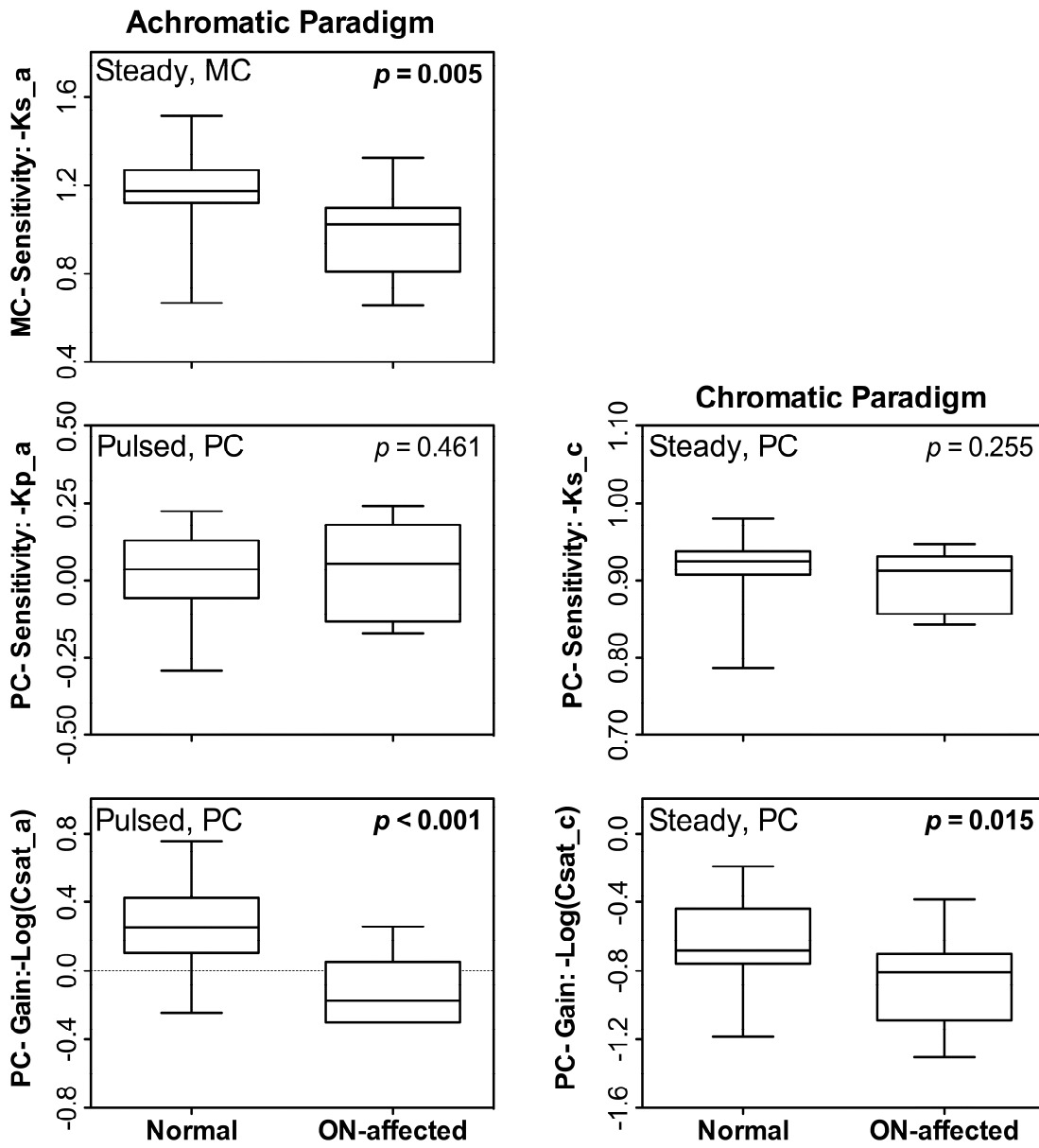
Figure 1:

Figure 2

Figure 3:

Figure 4

Table 1: Clinical characteristics of ON patients

ON Patient	Sex	Age(y)	OD				OS				MS
			BVA	HVF (MD)	ON	Onset Year	BVA	HVF (MD)	ON	Onset Year	
P1	F	42	20/20	-3.29	Yes	2006	20/20	-4.6	Yes	2006	Unknown
P2	F	29	20/25	-2.43	Yes	2000	20/25	-1.8	Yes	2000	Yes
P3	F	26	20/25	-1.16	Yes	2005	20/20	-0.81	No	--	Yes
P4	F	29	20/20	-2.97	Yes	2005	20/20	-3.65	Yes	2005	Yes
P5	F	30	20/25	-3.52	Yes	1998	20/25	-1.19	Yes	2002	Yes
P6	F	56	20/25	-0.14	Yes	2006	20/25	0.82	Yes	2006	No
P7	M	40	20/50	-3.52	Yes	1993	20/20	-2.24	Yes	2004	Yes
P8	F	34	20/20	0.48	Yes	2007	20/20	-0.54	No	--	Yes
P9	F	32	20/20	-0.1	Yes	2008	20/20	-1.32	Yes	2008	No
P10	F	55	20/20	-1.25	No	--	20/25	-1.87	Yes	2004	Unknown
P11	M	47	20/30	-1.94	Yes	2008	20/20	-2.77	Yes	2008	Yes